Key Points:
- We calibrate coefficients from earthquake early warning methodologies to do a fast estimation of magnitude for subduction earthquakes
- These methodologies are able to robustly estimate the magnitude for small-to-moderate events (Mw ≤ 7.0) ~30 from origin time
- Large events (Mw ≥ 7.5) required data from GNSS to perform the magnitude estimation ~70 s from origin time

Supporting Information:
- Supporting Information S1

Correspondence to:
F. Leyton,
leyton@csn.uchile.cl

How Fast Can We Reliably Estimate the Magnitude of Subduction Earthquakes?

F. Leyton[1] (iD), S. Ruiz[2] (iD), J. C. Baez[1] (iD), G. Meneses[3], and R. Madariaga[3] (iD)

[1]Centro Sismológico Nacional, Universidad de Chile, Santiago, Chile, [2]Departamento de Geofísica, Universidad de Chile, Santiago, Chile, [3]Laboratoire de Géologie, CNRS, University Paris Science Letters and Ecole Normale Supérieure, Paris, France

Abstract Fast and reliable characterization of earthquakes can provide vital information to the population, even reducing the effects of strong shaking produced by them. In this study, we explore the minimum time required to estimate the magnitude for subduction earthquakes. Using traditional *P* wave earthquake early warning parameters and considering a progressively increasing time window, we are able to estimate magnitude for subduction earthquakes ~30 s from the origin time (with an average residual of 0.01 ± 0.28). However, estimations for larger events (Mw ≥ 7.5) present larger errors (average residual of −0.70 ± 0.30). We complement our data with Global Navigational Satellite System observations for these events, enabling magnitude estimations ~70 s from the origin time (average residual of −0.42 ± 0.41). We propose that rapid estimations of magnitude should consider, initially, *P* waves in a progressively increasing time window, and complemented with GNSS data, for large events.

Plain Language Summary Fast and reliable magnitude estimation of earthquakes enables the preparation of the public to reduce its impact. Here we test known methods to rapidly estimate the magnitude of subduction earthquakes. We found encouraging results, taking a few tens of seconds to provide reliable values. However, results for larger events tend to underestimate the real magnitude. Hence, we propose the combination with other sources of information, such as Global Positioning System, that are able to resolve these larger events.

1. Introduction

Recent advances in communication and automatic processing of seismic data have enabled fast and reliable earthquake source estimation, improving the rapid response of public and private agencies as well as the general public (Kanamori, 2005; Satriano et al., 2011). Indeed, fast estimations of the location, magnitude, and expected ground motions are the basis of the present Earthquake Early Warning Systems (EEWS) aimed to prevent losses produced by earthquakes (Colombelli & Zollo, 2016; Heaton, 1985; Satriano et al., 2011). In general, these systems aim to provide a few seconds warning in advance of the destructive seismic waves of an earthquake, based on a continuous, real-time, seismic monitoring (Colombelli et al., 2015).

The main principle in usual EEWS is that the information from few seconds of the *P* wave can provide information regarding the magnitude and location of an earthquake (Allen & Kanamori, 2003), and given that these waves travel faster than the potentially destructive waves, this can provide an actionable warning to the population to reduce the impact of shaking (Colombelli & Zollo, 2016). However, there always will be a trade-off between the warning time and the reliability of the information: larger time windows should enable better knowledge of the event, while giving less time to prepare for its impact; this concept has lead to a general use of continuous updates in EEWS (Colombelli et al., 2012, 2015; Satriano et al., 2011). Moreover, Minson et al. (2018), using simple seismological relations, discussed the minimum time required to estimate the possibility of having strong ground shaking due to an earthquake: they showed that there is a limit given by the required time for the earthquake to evolve into a large event.

Indeed, a key aspect that remains controversial is whether a few seconds of the *P* wave can predict the earthquake's size over a wide range of magnitudes: some authors suggest that an initial rupture will develop into a large earthquake only if it has enough fracture energy to break across several heterogeneities (Olson & Allen, 2005). In this case, the Deterministic model, the final seismic moment is determined by the initial rupture (Ellsworth & Beroza, 1995; Zollo et al., 2006). However, as pointed out by Rydelek & Horiuchi (2006), it is not clear by which mechanism the information between these heterogeneities is transmitted across large
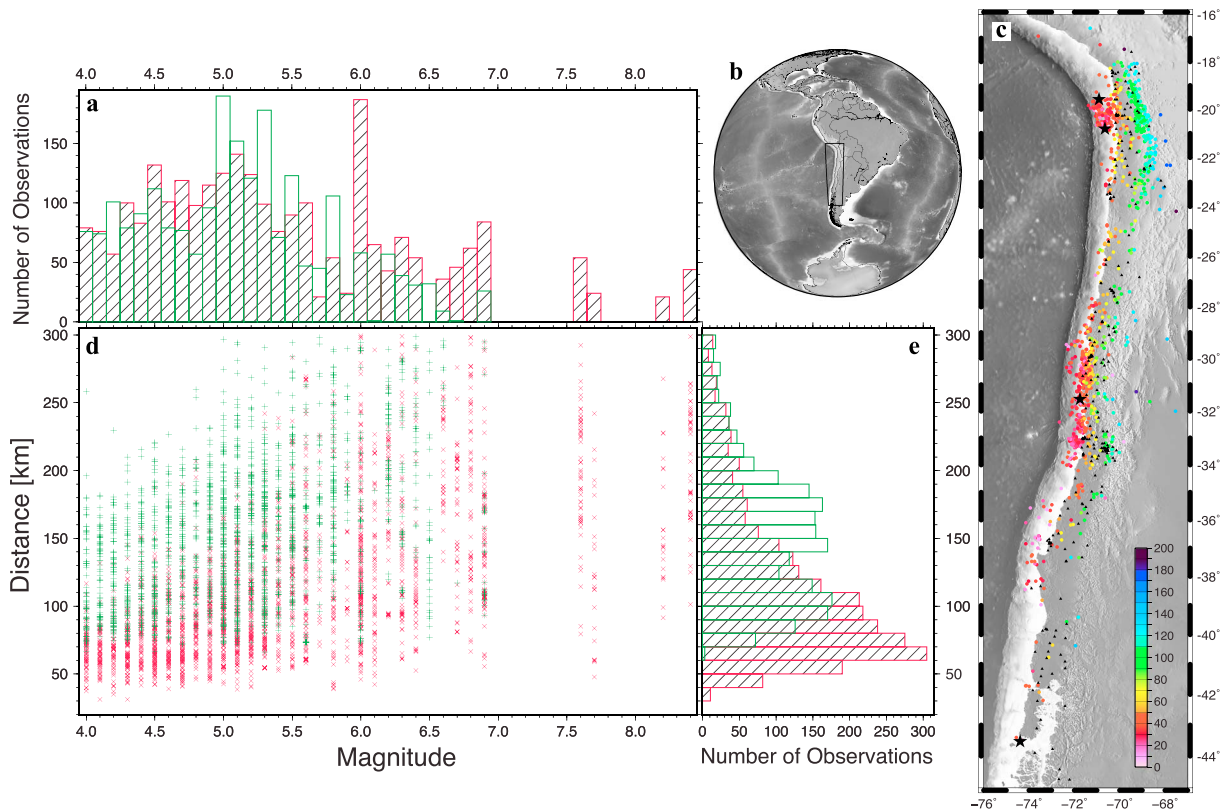
Figure 1. Data from the Chilean Strongmotion Database used in this study. Panel c presents a map with the location of the events (colored circles); the color is proportional to the depth, following the scale on the lower right corner. The stars show the epicenters of the largest events in the database (magnitude Mw ≥ 7.5), presented in panels c to f in Figure 4. Panel b shows a global map with the specified study area. Panel d shows the distribution of the records with respect to magnitude and hypocentral distance, while panels a and e present the corresponding histograms. For panels a, d, and e, the red crosses are used for interplate events, while the green plus signs are used for intermediate-depth, intraplate events.

distances (from tens to hundreds of kilometers). In other words, the first few seconds of the *P* wave cannot capture the entire process of a large earthquake (Festa et al., 2008). Hence, the interpretation that ruptures of large-magnitude events are deterministic is strongly disputed (Colombelli et al., 2014); even more, Meier et al. (2016) found no difference in the onset of events ranging from magnitudes 4.0 up to 8.0, suggesting that the propagation of rupture into a large earthquake is not defined by the initial part of the *P* wave, supporting the Cascade model (Ellsworth & Beroza, 1995).

Recently, given the availability of real-time Global Navigation Satellite System (GNSS) data, it has been proposed to include it into EEWS, enabling the fast characterization of moderate-to-large events (Allen & Ziv, 2011; Colombelli et al., 2013; Crowell et al., 2009). Furthermore, Crowell et al. (2013) proposed the use of the peak ground displacement (PGD) directly measured from the three-component GNSS time series to estimate the magnitude for these events (see also Melgar et al., 2015). While GNSS data are noisier than traditional seismic data, it is capable of capturing the full displacement history of an event without filtering, lending itself well to modeling the total moment release of moderate-to-large earthquakes in the near field (Melgar et al., 2015).

In the present study, we take advantage of the recently deployed seismological and geodetic stations from the Centro Sismológico Nacional (Barrientos & National Seismological Center (CSN) Team, 2018; Leyton et al., 2018a; Báez et al., 2018); these networks have successfully recorded large-magnitude, subduction earthquakes in the near field (Leyton et al., 2018b), among them, the 2014 Iquique (Mw 8.2) and its largest aftershock (Mw 7.7), the 2015 Illapel (Mw 8.3), and the 2016 Chiloé (Mw 7.6; shown as black stars in Figure 1c). We use these data, considering first the early portion of the *P* wave from strong motion records, to estimate the magnitude of the event, as done in traditional EEWS: the high-pass-filtered peak displacement amplitude, the predominant period, the characteristic period, and the integral of the squared velocity (for a recent review,

see Colombelli & Zollo, 2016). Later, we extend these computations to consider the complete *P* wave (up to the *S* wave arrival) in a progressively increasing fashion (Colombelli et al., 2012, 2015). Finally, we complement these results with estimations of magnitude from GNSS data, addressing the question: how fast can we estimate the magnitude of subduction earthquakes?

2. Data and Methods

2.1. Data

In the present study, we use data from events of the Chilean subduction zone, from 2012 up to April 2018, for events of magnitude 4.0 and above, recorded at hypocentral distances less than 300 km (Leyton et al., 2018b). Here we separated the most common seismic source found in the Chilean Subduction zone: (1) interplate and (2) intermediate-depth, intraplate events (Ruiz & Madariaga, 2018), considering the hypocenter and the relative slab location, allowing an error of 20 km in depth. In this database, we collected 2,605 records for interplate earthquakes and 2,152 for intermediate-depth, intraplate events; the distribution of the records that we used is presented in Figure 1. From this figure, we observe that most of the data correspond to interplate events with hypocentral distances less than 100 km and magnitudes less than 6.0.

All records correspond to accelerograms from the Chilean Strongmotion Network; see the Acknowledgments section and Figure S1 of the supporting information for details (Leyton et al., 2018a). All traces were processed the same way: we removed the instrument response, in the frequency domain; removed the trend; high-pass filter the data (corner frequency of 0.075 Hz) in the frequency domain, and, finally, integrate the data into velocity, in the time domain. In case the data were needed in ground displacement, this new integration was performed again in the time domain.

2.2. Methods

We apply the traditional parameters that can be measured in real-time seismology, usually used in EEWS, considering only *P* wave from strong motion records. In this study, we used the high-pass-filtered peak displacement amplitude (Pd; Wu & Zhao, 2006; Zollo et al., 2006), the predominant period (τ_p; Allen & Kanamori, 2003; Nakamura, 1984, 1988), the characteristic period (τ_c; Kanamori, 2005), and the integral of the squared velocity (Iv2; Festa et al., 2008), all of them previously applied in Chile for the Tocopilla 2007 earthquake sequence (Lancieri et al., 2011). Some results are shown in Figures 2a–2d. These results were computed considering a 4-s, *P* wave time window (PTW). Upper panels present the results of the general relation:

$$\log (\text{PAR}) = A + B^*M \tag{1}$$

where PAR is one of the selected parameters (Pd, τ_p, τ_c, or Iv2), *M* corresponds to the magnitude, and *A* and *B* are coefficients to be determined. In this case, Pd and Iv2 have been corrected to a reference distance of 1 km, as done in similar studies (Zollo et al., 2006), using the following relation:

$$\log (\text{Pd}_{r=1\text{km}}) = \log (\text{Pd}|_{r=R}) - C \log (R). \tag{2}$$

The coefficients (*A*, *B*, and *C*) were computed by a least squares method (Zollo et al., 2006); results can be found in Table S1a. Figure 2 also shows a comparison of the predicted magnitude as a function of magnitude (lower panels): the red circles represent the mean value, with whiskers representing the corresponding standard deviation; each cross represents a single estimation (i.e., one station for a single event). The green lines in all panels show the estimated relation, considering only events of magnitude less than 7.0. The results show that Pd and Iv2 have smaller standard deviations than τ_p and τ_c, also seen by Lancieri et al. (2011). The corresponding results for intermediate-depth, intraplate events are presented in Figures S2a to S2d. For this data set, the behavior is similar to that of interplate events: there are smaller errors for Pd and Iv2, compared to those of τ_p and τ_c. Also note that the scaling of the different parameters is reliable up to magnitude ~7.0, as seen in previous studies for other geodynamic contexts (Kanamori, 2005; Rydelek & Horiuchi, 2006; Rydelek et al., 2007; Colombelli et al., 2012): for low-to-moderate magnitude events (magnitude ≤7.0), the average residual (difference between the observed and estimated magnitude) is 0.01 ± 0.28, ~30 s after origin time; while for larger events (magnitude >7.0), the average residual is −0.70 ± 0.30, ~70 s after origin time (see Tables S3 and S5 of the supporting information).
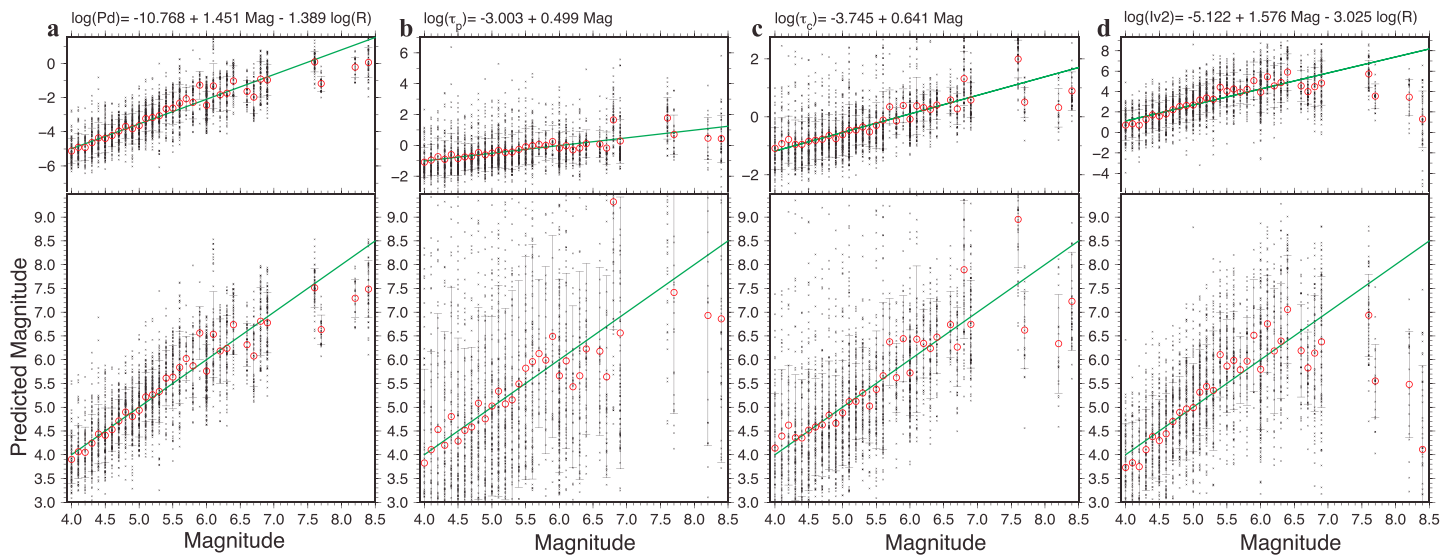
Figure 2. Results of the relation of the earthquake early warning (EEW) parameters as a function of magnitude (top panels): high-pass-filtered peak displacement (Pd), predominant period (τ_p), characteristic period (τ_c), and integral of the squared velocity (Iv2), for panels a to d, respectively. Bottom panels show the results converted into the predicted magnitude. For all panels, the red circles show the average for each magnitude, while the black whiskers show the standard deviation; the green lines show the resulting correlation, considering events Mw ≤ 7.0 and a 4-s *P* wave time window. All coefficients are listed in Tables S1a to S2d of the supporting information.

Following Colombelli et al. (2012, 2015), we considered a progressively increasing PTW, up to the *S* wave time arrival. Hence, we determined the required coefficients (*A*, *B*, and *C*) for different PTW starting from 2 up to 35 s, limited by the arrival of the *S* wave. We also computed the weighted standard error (WSE), as suggested by Zollo et al. (2006); all values are presented in Tables S1a to S2d of the supporting information. From these tables, we find that all coefficients change up to ~20 s, probably due to the time required to record the complete source time function; even more, this indicates that no clear improvements are achieved by considering longer PTW. In order to reproduce the conditions of real-time computations, the considered body wave time arrivals (*P* and *S* waves) were computed from theoretical models, using TauP method (Crotwell et al., 1999).

The results for Pd are shown in Figure 3, while other results can be found in Figures S2a to S2c. Note the reduction in the standard deviation (whiskers in Figure 3) as the PTW increases. This suggests that the prediction of magnitude will improve with increasing PTW, for the magnitude range considered. The results for intermediate-depth, intraplate events follow a similar behavior, showing a clear decrease in error with the increase of the time window from the *P* wave arrival, as can be seen in Figures S2a to S2d (for Pd, τ_p, τ_c, and Iv2, respectively).

3. Results

First, we tested how we could estimate the magnitude considering the methodologies previously described, considering only *P* waves up to the arrival of the *S* wave. We followed an evolutionary approach, as recently proposed by Caprio et al. (2011) and Colombelli et al. (2012, 2015), and used different PTW to make the estimation, updated every second; in other words, for each point in time, we considered the coefficients given the corresponding *P* wave time window. Nevertheless, by analyzing Figure 3 we noticed changes in the resulting errors (and WSE shown in Tables S1a to S2d), reducing to almost a half for a PTW of 10 s. Hence, we decided to take into account this feature and include the resulting WSE as an inverse weight in the new computations. Some examples are presented in blue in Figures 4, S3a, and S3b, while in green are shown the results of the magnitude estimation using the PGD from GNSS data (Crowell et al., 2013; Melgar et al., 2015); the whiskers represent the estimated errors (standard deviation) for each point, and the height of the rectangle is proportional to the number of GNSS stations considered. The PGD methodology has been tested in Chile for large events (Crowell, Schmidt, et al., 2018; Báez et al., 2018), nevertheless, results that could be improved considering a local PGD regression instead a global estimation of Melgar et al. (2015),
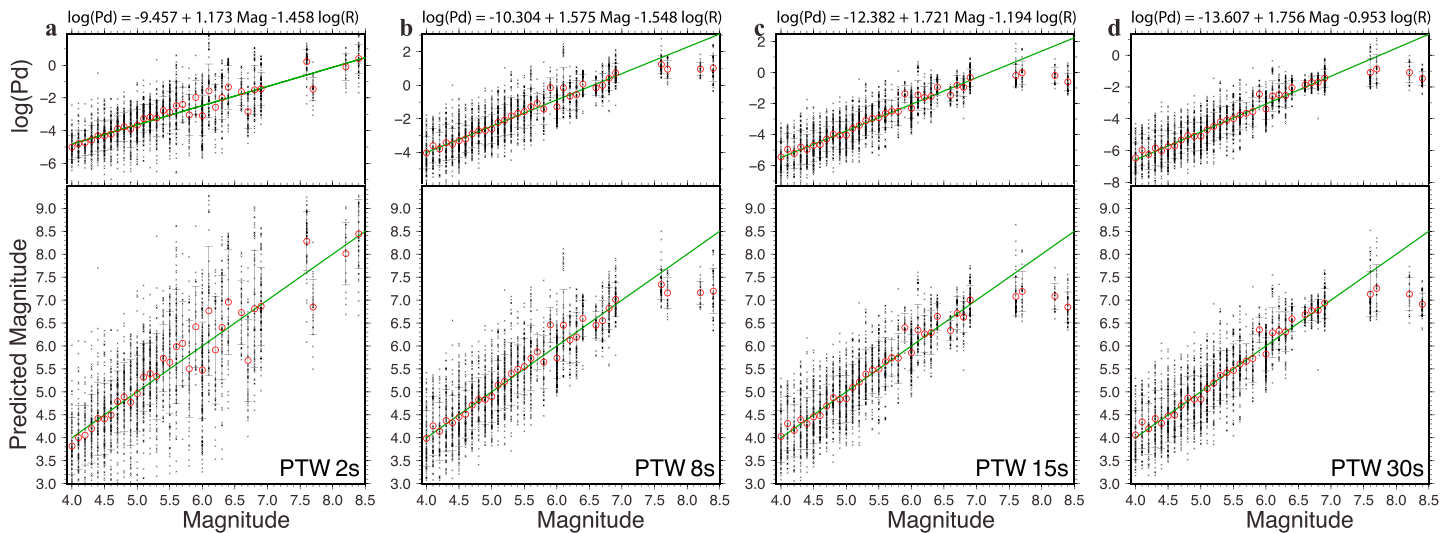
Figure 3. Results of the peak displacement (Pd) as a function of magnitude, for different *P* wave time window (PTW). For panels a to d we considered PTW of 2, 8, 15, and 30 s, respectively; all symbols and colors are the same as described in Figure 2.

used in this work. In the present study, we have considered results of GNSS time series computed using corrected orbits only, reproducing CSN's real-time conditions (Báez et al., 2018). In this case, we computed the displacements relative to the position 10 min before the origin time.

Note that the first estimations present large errors, probably because in the first few seconds there are few observations and their estimated magnitudes present large errors. Afterward, as the time advances, the estimations improve and errors reduced, falling from 0.4–0.5 to 0.1–0.2. For larger magnitudes (Mw 7.0 and above), the estimations become increasingly irregular: for a magnitude 7.6 (Chiloé 2016 earthquake, shown in panel c), it starts with the usual overestimation, decrease to a value close to the exact, to end with a slightly higher estimation. However, for the three large subduction thrust events (main aftershock of the Iquique 2014 event, mainshock Iquique 2014, and Illapel 2015 earthquake, shown in panels d, e, and f, magnitude 7.7, 8.2, and 8.3, respectively) the estimates are poorly constrained: they start with large errors, to end up with an estimated magnitude ~7.0; these differences are probably due to the nucleation phase observed in larger events (Ruiz et al., 2014, 2016), as discussed in section 5. The GNSS stations used in each case, along with more results supporting these observations, can be found in Figures S5 and S4a and S4b (for interplate and intermediate-depth, intraplate events, respectively).

To evaluate the performance of each method, we fitted the residuals (difference between the observed and estimated magnitude) with a normal distribution, with a 95% confidence interval, obtaining the average and standard deviation for each case; all values are presented in Tables S3–S5 of the supporting information, as a function of time after the origin. From these values, we found that after ~30 s from origin time, Pd gives a robust estimation for small-to-moderate magnitude interplate events (magnitudes ≤ 7.0), with average residual of 0.01 ± 0.28. On the other hand, for larger events (magnitudes > 7.0), we fail to obtain a reliable estimation, with an average residual of −0.70 ± 0.30, ~70 s after the origin. On the other hand, for the same time lapse (~70 s after origin) using PGD from GNSS data, we are able to estimate the magnitude with an average residual of −0.42 ± 0.41, see details in Tables S3–S5 of the supporting information. Note that, in both cases, the obtained magnitudes are underestimated, as can be seen from the negative average residual.

4. Discussions

The fast estimation of magnitude represents a corner stone in most of Early Warning Systems, aiming to retrieve reliable values within a few minutes from the earthquake origin time, in order to provide an alert to the public. In this study, we explore the capabilities that the *P* wave offers to provide information to enable a robust estimation. For most cases, for interplate events of magnitude 7.0 and below, the methodologies enable a robust estimation of the magnitude ~30 s from the origin time (average residual of 0.01 ± 0.28);
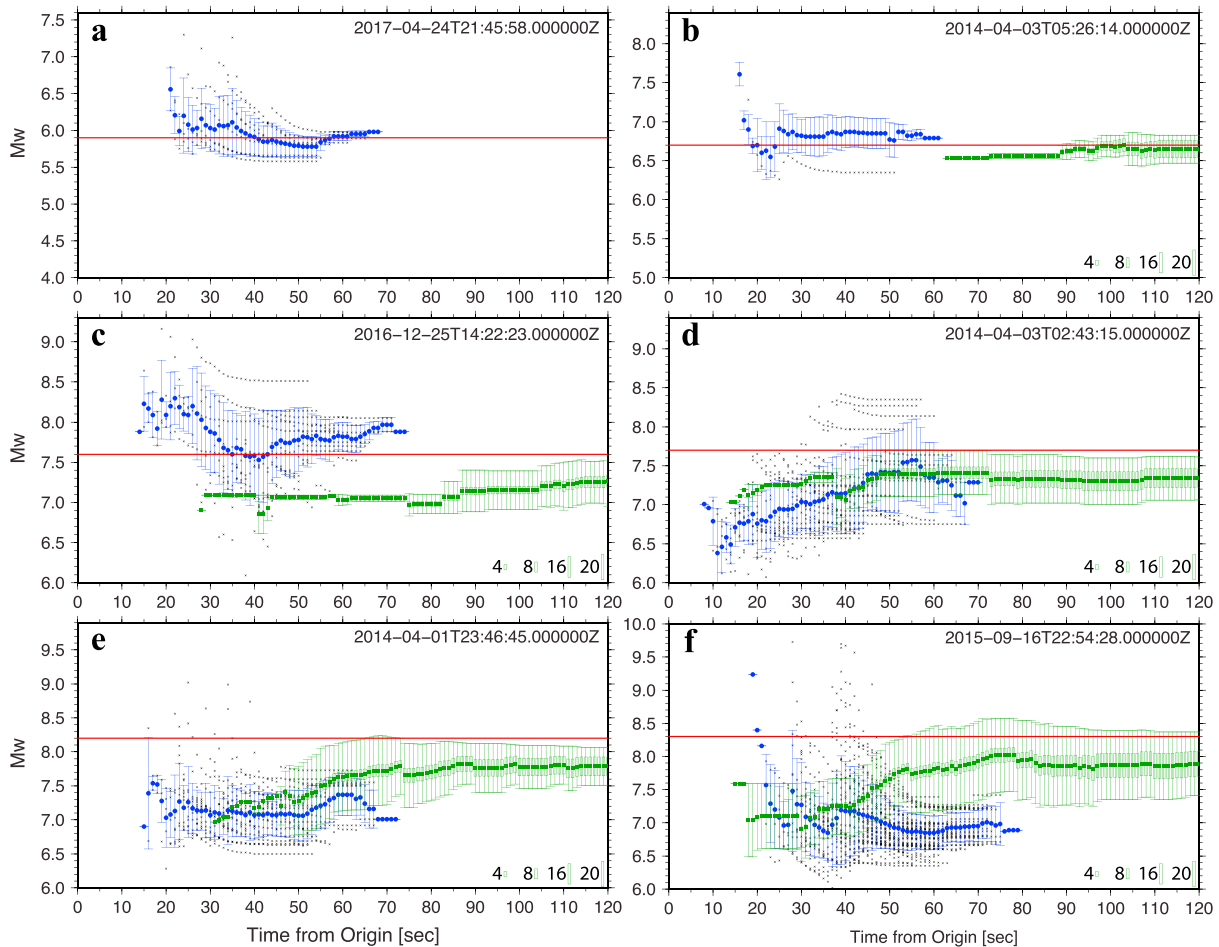
Figure 4. Results of fast magnitude estimation for some interplate earthquakes using low-pass-filtered peak displacement (Pd) from strong motion records (blue) and peak ground displacement (PGD) from GNSS data (green); the vertical whiskers represent in the error in each case, and the height of the green rectangle is proportional to the number of GNSS stations considered, following the symbols of the lower, right corner. The small black crosses are the individual estimations of a single station, using Pd; the horizontal red line marks the real magnitude. In the upper, right corner of each panel we show the UTC date and time of the event.

similar results were found for intermediate-depth, intraplate earthquakes (average residual of 0.00 ± 0.43). However, for larger events, magnitude 7.5 and above, these estimates become less reliable (average residual of −0.70 ± 0.30), ~70 s after origin.

Nevertheless, for large events, the GNSS systems provide useful information that enable robust magnitude estimation within the first couple of minutes from the origin time (average residual of −0.42 ± 0.41, 70 s after origin); similar results were found for earthquakes in Japan and California by Colombelli et al. (2013). This is due to the fact that GNSS systems are still not able to precisely record the early *P* waves, recording only the largest portion of the shaking, as shown in Figure 5, probably due to the noise levels that currently real-time GNSS time series present. From this figure, we can see that in all cases, the GNSS is able to record only the second portion of the shaking, after the *S* wave arrival, as has been pointed out (Allen & Ziv, 2011). Hence, independent from the network geometry for a specific case, strong motion stations (using *P* wave methods) will always be able to provide faster magnitude estimates, but it might be an underestimation for large events (Mw ≥ 7.5). On the other hand, GNSS systems required a longer time window in order to provide useful data; however, these estimations will be more accurate, providing a better estimation of the magnitude for large events (Allen & Ziv, 2011). Here based on the data analyzed, we propose to consider time windows of ~30 and ~70 s from origin time, for Pd and PGD, respectively, but more detailed studies should better constrain these values. Nevertheless, these longer time windows can still provide an alert to the population: for some localities, it takes more than 80 s for the strong shaking to reach it (see Figure S5 of
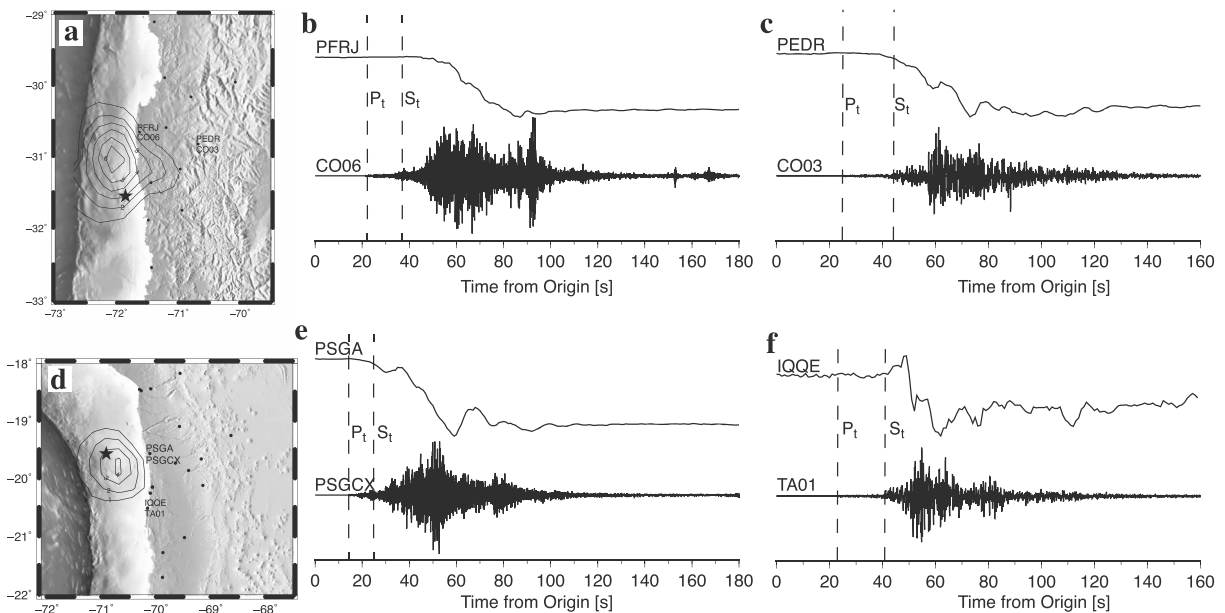
Figure 5. Comparison of strong motion and GNSS east–west time series (recorded at stations with collocated accelerometer and GNSS antenna), for the 2015 Illapel (Mw 8.3; top) and 2014 Iquique (Mw 8.2; bottom) earthquakes. Left panels (a and d) show a map with contour lines of dislocation models, from Ruiz et al. (2014, 2016); the black stars mark the epicenter and the black circles the stations. Selected stations are marked by the corresponding station code. In panels b, c, e, and f, we marked the P and S wave time arrival, P_t and S_t, respectively, with vertical, dashed lines.

the supporting information), giving some seconds for the alert to be issued, as observed in other cases (Crowell, Melgar, & Geng, 2018).

Even though it has been suggested that hypocenter and the location of the peak slip in the fault are statistically close (Mai et al., 2005) or not independent (Olson & Allen, 2006), the examples shown in Figure 5 show no clear correlation between them. In fact, 2015 Illapel (Mw 8.3) and 2014 Iquique (Mw 8.2) earthquakes present nucleation phases of ~20 and ~30 s, respectively, only observable in the strong motion data (Ruiz et al., 2014, 2016). This complex nucleation could explain the difficulties to extend the observations from low-to-moderate magnitude events to those with magnitude above 7.0; moreover, this complexity has been suggested as responsible for the failure of traditional EEW parameters, as in the case of the 2011 Tohoku-Oki earthquake (Colombelli & Zollo, 2016). Nevertheless, as suggested by Rydelek et al. (2007), we believe that the analysis of P wave can still be useful to issue a warning that a large earthquake has occurred, given that some threshold have been exceeded in the network.

5. Conclusions

The saturation of EEW parameters is due to, at least, the following: (1) the limited portion of the P wave that can be analyzed in the near field, given the prompt arrival of the S wave (Colombelli et al., 2013), and (2) complex nucleation of large-magnitude events. Nevertheless, for the events studied here, we require ~30 s to estimate the magnitude of an event Mw ≤ 7.0 (with an average residual of 0.10 ± 0.28); for larger events, longer time windows are required, as discussed in Minson et al. (2018). In our case, considering GNSS data and its station's geometry, ~70 s time window is required to get a robust estimation of magnitude. In the present study, GNSS data severely underestimate the magnitude (average residual of −0.42 ± 0.41, ~70 s from origin time), probably due to the use of a global regression instead of a local one, as previously discussed, and availability of data in CSN's real-time conditions.

Given the performance of usual EEW parameters and GNSS data, for subduction earthquakes, we propose a strategy composed by two data sets: triggering and first location should come from seismic data, giving a preliminary magnitude and, in case it exceeds a given threshold (e.g., Mw 6.5), systems should consult the GNSS streams to look for clues of a large event.

References

Allen, R. M., & Kanamori, H. (2003). The potential for earthquake early warning in southern California. *Science*, *300*(5620), 786–789. https://doi.org/10.1126/science.1080912

Allen, R. M., & Ziv, A. (2011). Application of real-time GPS to earthquake early warning. *Geophysical Research Letters*, *38*, L16310. https://doi.org/10.1029/2011GL047947

Báez, J. C., Leyton, F., Troncoso, C., del Campo, F., Bevis, M., Vigny, C., et al. (2018). The Chilean GNSS network: Current status and progress toward early warning applications. *Seismological Research Letters*, *89*, 1546–1554. https://doi.org/10.1785/0220180011

Barrientos, S., & National Seismological Center (CSN) Team (2018). The seismic network of Chile. *Seismological Research Letters*, *89*(2A), 467–474.

Caprio, M., Lancieri, M., Cua, G. B., Zollo, A., & Wiemer, S. (2011). An evolutionary approach to real-time moment magnitude estimation via inversion of displacement spectra. *Geophysical Research Letters*, *38*, L02301. https://doi.org/10.1029/2010GL045403

Colombelli, S., Allen, R. M., & Zollo, A. (2013). Application of real-time GPS to earthquake early warning in subduction and strike-slip environments. *Journal of Geophysical Research: Solid Earth*, *118*, 3448–3461. https://doi.org/10.1002/jgrb.50242

Colombelli, S., Caruso, A., Zollo, A., Festa, G., & Kanamori, H. (2015). A P wave-based, on-site method for earthquake early warning. *Geophysical Research Letters*, *42*, 1390–1398. https://doi.org/10.1002/2014GL063002

Colombelli, S., & Zollo, A. (2016). Rapid and reliable seismic source characterization in earthquake early warning systems: Current methodologies, results, and new perspectives. *Journal of Seismology*, *20*(4), 1171–1186. https://doi.org/10.1007/s10950-016-9570-z

Colombelli, S., Zollo, A., Festa, G., & Kanamori, H. (2012). Early magnitude and potential damage zone estimates for the great Mw 9 Tohoku-Oki earthquake. *Geophysical Research Letters*, *39*, L22306. https://doi.org/10.1029/2012GL053923

Colombelli, S., Zollo, A., Festa, G., & Picozzi, M. (2014). Evidence for a difference in rupture initiation between small and large earthquakes. *Nature Communications*, *5*(1), 3958. https://doi.org/10.1038/ncomms4958

Crotwell, H. P., Owens, T. J., & Ritsema, J. (1999). The TauP Toolkit: Flexible seismic travel-time and ray-path utilities. *Seismological Research Letters*, *70*(2), 154–160. https://doi.org/10.1785/gssrl.70.2.154

Crowell, B. W., Bock, Y., & Squibb, M. B. (2009). Demonstration of earthquake early warning using total displacement waveforms from real-time GPS networks. *Seismological Research Letters*, *80*(5), 772–782. https://doi.org/10.1785/gssrl.80.5.772

Crowell, B. W., Melgar, D., Bock, Y., Haase, J. S., & Geng, J. (2013). Earthquake magnitude scaling using seismogeodetic data. *Geophysical Research Letters*, *40*, 6089–6094. https://doi.org/10.1002/2013GL058391

Crowell, B. W., Melgar, D., & Geng, J. (2018). Hypothetical real-time GNSS modeling of the 2016 Mw 7.8 Kaikōura earthquake: Perspectives from ground motion and tsunami inundation prediction. *Bulletin of the Seismological Society of America*, *108*(3B), 1736–1745. https://doi.org/10.1785/0120170247

Crowell, B. W., Schmidt, D. A., Bodin, P., Vidale, J. E., Baker, B., Barrientos, S., & Geng, J. (2018). G-FAST earthquake early warning potential for great earthquakes in Chile. *Seismological Research Letters*, *89*(2A), 542–556. https://doi.org/10.1785/0220170180

Ellsworth, W. L., & Beroza, G. C. (1995). Seismic evidence for an earthquake nucleation phase. *Science*, *268*(5212), 851–855. https://doi.org/10.1126/science.268.5212.851

Festa, G., Zollo, A., & Lancieri, M. (2008). Earthquake magnitude estimation from early radiated energy. *Geophysical Research Letters*, *35*, L22307. https://doi.org/10.1029/2008GL035576

Heaton, T. H. (1985). A model for a seismic computerized alert network. *Science*, *228*(4702), 987–990. https://doi.org/10.1126/science.228.4702.987

Kanamori, H. (2005). Real-time seismology and earthquake damage mitigation. *Annual Review of Earth and Planetary Sciences*, *33*(1), 195–214. https://doi.org/10.1146/annurev.earth.33.092203.122626

Lancieri, M., Fuenzalida, A., Ruiz, S., & Madariaga, R. (2011). Magnitude scaling of early-warning parameters for the M w 7.8 Tocopilla, Chile, earthquake and its aftershocks. *Bulletin of the Seismological Society of America*, *101*(2), 447–463. https://doi.org/10.1785/0120100045

Leyton, F., Leopold, A., Hurtado, G., Pastén, C., Ruiz, S., Montalva, G., & Sáez, E. (2018a). Geophysical characterization of the Chilean seismological stations: First results. *Seismological Research Letters*, *89*(2A), 519–525. https://doi.org/10.1785/0220170156

Leyton, F., Pastén, C., Ruiz, S., Idini, B., & Rojas, F. (2018b). Empirical site classification of CSN network using strong-motion records. *Seismological Research Letters*, *89*(2A), 512–518. https://doi.org/10.1785/0220170167

Mai, P. M., Spudich, P., & Boatwright, J. (2005). Hypocenter locations in finite-source rupture models. *Bulletin of the Seismological Society of America*, *95*(3), 965–980. https://doi.org/10.1785/0120040111

Meier, M. A., Heaton, T., & Clinton, J. (2016). Evidence for universal earthquake rupture initiation behavior. *Geophysical Research Letters*, *43*, 7991–7996. https://doi.org/10.1002/2016GL070081

Melgar, D., Crowell, B. W., Geng, J., Allen, R. M., Bock, Y., Riquelme, S., et al. (2015). Earthquake magnitude calculation without saturation from the scaling of peak ground displacement. *Geophysical Research Letters*, *42*, 5197–5205. https://doi.org/10.1002/2015GL064278

Minson, S. E., Meier, M. A., Baltay, A. S., Hanks, T. C., & Cochran, E. S. (2018). The limits of earthquake early warning: Timeliness of ground motion estimates. *Science Advances*, *4*(3), eaaq0504. https://doi.org/10.1126/sciadv.aaq0504

Nakamura, Y. (1984). Development of earthquake early-warning system for the Shinkansen, some recent earthquake engineering research and practical in Japan. *The Japanese National Committee of the International Association for Earthquake Engineering, Tokyo, Japan*, (pp. 224–238).

Nakamura, Y. (1988). On the urgent earthquake detection and alarm system (UrEDAS). In *Proc. of the 9th World Conference on Earthquake Engineering*, (Vol. 7, pp. 673–678). Japan: Tokyo-Kyoto.

Olson, E. L., & Allen, R. M. (2005). The deterministic nature of earthquake rupture. *Nature*, *438*(7065), 212–215. https://doi.org/10.1038/nature04214

Olson, E. L., & Allen, R. M. (2006). Earth science: Is earthquake rupture deterministic? (reply). *Nature*, *442*(7100), E6. https://doi.org/10.1038/nature04964

Ruiz, S., Klein, E., del Campo, F., Rivera, E., Poli, P., Metois, M., et al. (2016). The seismic sequence of the 16 September 2015 M w 8.3 Illapel, Chile, earthquake. *Seismological Research Letters*, *87*(4), 789–799. https://doi.org/10.1785/0220150281

Ruiz, S., & Madariaga, R. (2018). Historical and recent large megathrust earthquakes in Chile. *Tectonophysics*, *733*, 37–56. https://doi.org/10.1016/j.tecto.2018.01.015

Ruiz, S., Metois, M., Fuenzalida, A., Ruiz, J., Leyton, F., Grandin, R., et al. (2014). Intense foreshocks and a slow slip event preceded the 2014 Iquique Mw 8.1 earthquake. *Science*, *345*(6201), 1165–1169. https://doi.org/10.1126/science.1256074

Rydelek, P., & Horiuchi, S. (2006). Earth science: Is earthquake rupture deterministic? *Nature*, *442*(7100), E5.

Rydelek, P., Wu, C., & Horiuchi, S. (2007). Comment on "Earthquake magnitude estimation from peak amplitudes of very early seismic signals on strong motion records" by Aldo Zollo, Maria Lancieri, and Stefan Nielsen. *Geophysical Research Letters*, *34*, L20302. https://doi.org/10.1029/2007GL029387

Satriano, C., Wu, Y. M., Zollo, A., & Kanamori, H. (2011). Earthquake early warning: Concepts, methods and physical grounds. *Soil Dynamics and Earthquake Engineering*, *31*(2), 106–118. https://doi.org/10.1016/j.soildyn.2010.07.007

Wessel, P., & Smith, W. H. (1998). New, improved version of Generic Mapping Tools released. *Eos, Transactions American Geophysical Union*, *79*(47), 579–579. https://doi.org/10.1029/98EO00426

Wu, Y. M., & Zhao, L. (2006). Magnitude estimation using the first three seconds *P*-wave amplitude in earthquake early warning. *Geophysical Research Letters*, *33*, L16312. https://doi.org/10.1029/2006GL026871

Zollo, A., Lancieri, M., & Nielsen, S. (2006). Earthquake magnitude estimation from peak amplitudes of very early seismic signals on strong motion records. *Geophysical Research Letters*, *33*, L23312. https://doi.org/10.1029/2006GL027795